

# Nonlinear left-handed metamaterials

Ilya V. Shadrivov<sup>1</sup>, Alexander A. Zharov<sup>1,2</sup>, Nina A. Zharova<sup>1,3</sup>, and Yuri S. Kivshar<sup>1</sup>

<sup>1</sup>*Nonlinear Physics Centre, Research School of Physical Sciences and Engineering,  
Australian National University, Canberra ACT 0200, Australia*

<sup>2</sup>*Institute for Physics of Microstructures, Russian Academy of Sciences, Nizhny Novgorod 603950, Russia*

<sup>3</sup>*Institute of Applied Physics, Russian Academy of Sciences, Nizhny Novgorod 603600, Russia*

We analyze nonlinear properties of microstructured materials with negative refraction, the so-called left-handed metamaterials. We demonstrate that the hysteresis-type dependence of the magnetic permeability on the field intensity allows changing the material properties from left- to right-handed and back. Using the finite-difference time-domain simulations, we study wave transmission through the slab of nonlinear left-handed material, and predict existence of temporal solitons in such materials. We demonstrate also that nonlinear left-handed metamaterials can support both TE- and TM-polarized self-trapped localized beams, spatial electromagnetic solitons. Such solitons appear as single- and multi-hump beams, being either symmetric or antisymmetric, and they can exist due to the hysteresis-type magnetic nonlinearity and the effective domains of negative magnetic permeability.

PACS numbers:

## I. INTRODUCTION

Recent theoretical studies [1, 2, 3] and experimental results [4, 5, 6] have shown the possibility of creating novel types of microstructured materials that demonstrate the property of negative refraction. In particular, the composite materials created by arrays of wires and split-ring resonators were shown to possess a negative real part of the magnetic permeability and dielectric permittivity for microwaves. These materials are often referred to as *left-handed materials* (LHMs) or *materials with negative refraction*. Properties of such materials were analyzed theoretically by Veselago a long time ago [7], but they were demonstrated experimentally only recently. As was shown by Veselago [7], left-handed materials possess a number of peculiar properties, including negative refraction for interface scattering, inverse light pressure, and reverse Doppler and Vavilov-Cherenkov effects.

So far, most of the properties of left-handed materials were studied in the linear regime of wave propagation when both the magnetic permeability and the dielectric permittivity of the material are assumed to be independent on the intensity of the electromagnetic field. However, any future effort in creating *tunable structures* where the field intensity changes the transmission properties of the composite structure would require the knowledge of nonlinear properties of such metamaterials, which may be quite unusual. In particular, the recently fabricated metamaterials consist of arrays of wires and split-ring resonators (SRRs). The array of wires provides negative dielectric permittivity, while SRRs give negative magnetic permeability. Metamaterials possess left-handed properties only in some finite frequency range, which is basically determined by the geometry of the structure. The possibility to control the effective parameters of the metamaterial using nonlinearity has recently been suggested in Refs. [8, 9]. Importantly, the microscopic electric field in the structure can be much higher

than the macroscopic electric field in the wave. This provides the mechanism for enhanced nonlinear effects.

In this paper we analyze nonlinear properties of left-handed metamaterials for the example of a lattice of the split-ring resonators and wires with a nonlinear dielectric. By means of finite-difference time-domain (FDTD) simulations we study the wave scattering on a slab of nonlinear composite structure. We also discuss the structure of electromagnetic solitons supported by the nonlinear left-handed materials with hysteresis-type nonlinear response. We believe that our findings may stimulate future experiments in this field, as well as studies of nonlinear effects in photonic crystals, where the phenomenon of negative refraction is analyzed now very intensively [10, 11].

## II. NONLINEAR RESONANT RESPONSE

We follow the original paper [8] and consider a two-dimensional composite structure consisting of a square lattice of the periodic arrays of conducting wires and split-ring resonators (SRR). We assume that the unit-cell size  $d$  of the structure is much smaller than the wavelength of the propagating electromagnetic field and, for simplicity, we choose the single-ring geometry of a lattice of cylindrical SRRs. The results obtained for this case are qualitatively similar to those obtained in the more involved cases of double SRRs. This type of microstructured materials has recently been suggested and built in order to create left-handed metamaterials with negative refraction in the microwave region [4].

The negative real part of the effective dielectric permittivity of such a composite structure appears due to the metallic wires whereas a negative sign of the magnetic permeability becomes possible due to the SRR lattice. As a result, these materials demonstrate the properties of negative refraction in the finite frequency band,

$\omega_0 < \omega < \min(\omega_p, \omega_{\parallel m})$ , where  $\omega_0$  is the eigenfrequency of the SRRs,  $\omega_{\parallel m}$  is the frequency of the longitudinal magnetic plasmon,  $\omega_p$  is an effective plasma frequency, and  $\omega$  is the angular frequency of the propagating electromagnetic wave,  $(\mathcal{E}, \mathcal{H}) \sim (\mathbf{E}, \mathbf{H}) \exp(i\omega t)$ . The split-ring resonator can be described as an effective LC oscillator (see, e.g. Ref. [12]) with the capacitance of the SRR gap, as well as an effective inductance and resistance.

Nonlinear response of such a composite structure can be characterized by two different contributions. The first one is an intensity-dependent part of the effective dielectric permittivity of the infilling dielectric. For simplicity, we may assume that the metallic structure is embedded into a nonlinear dielectric with a permittivity that depends on the intensity of the electric field in a general form,  $\epsilon_D = \epsilon_D(|\mathbf{E}|^2)$ . For results of calculations presented below, we take the linear dependence that corresponds to the Kerr-type nonlinear response.

The second contribution into the nonlinear properties of the composite material comes from the lattice of resonators, since the SRR capacitance (and, therefore, the SRR eigenfrequency) depends on the strength of the local electric field in a narrow slot. The intensity of the local electric field in the SRR gap depends on the electromotive force in the resonator loop, which is induced by the magnetic field. Therefore, the effective magnetic permeability  $\mu_{\text{eff}}$  depends on the macroscopic (average) magnetic field  $\mathbf{H}$ , and this dependence can be found in the form [8]

$$\mu_{\text{eff}}(\mathbf{H}) = 1 + \frac{F \omega^2}{\omega_{0NL}^2(\mathbf{H}) - \omega^2 + i\Gamma\omega}, \quad (1)$$

where

$$\omega_{0NL}^2(\mathbf{H}) = \left(\frac{c}{a}\right)^2 \frac{d_g}{[\pi h \epsilon_D(|\mathbf{E}_g(\mathbf{H})|^2)]}$$

is the eigenfrequency of oscillations in the presence of the external field of a finite amplitude,  $h$  is the width of the ring,  $\Gamma = c^2/2\pi\sigma ah$ , for  $h < \delta$ , and  $\Gamma = c^2/2\pi\sigma a\delta$ , for  $h > \delta$ . It is important to note that Eq. (1) has a simple physical interpretation: The resonant frequency of the artificial magnetic structure depends on the amplitude of the external magnetic field and, in turn, this leads to the intensity-dependent function  $\mu_{\text{eff}}$ .

Figures 1 and 2 summarize different types of nonlinear magnetic properties of the composite, which are defined by the dimensionless frequency of the external field  $\Omega = \omega/\omega_0$ , for both a *focusing* [Figs. 1, 2(a,b)] and a *defocusing* [Figs. 1, 2(c,d)] nonlinearity of the dielectric.

Due to the high values of the electric field in the slot of SRR as well as resonant interaction of the electromagnetic field with the SRR lattice, the characteristic magnetic nonlinearity in such structures is much stronger than the corresponding electric nonlinearity. Therefore, *magnetic nonlinearity should dominate* in the composite metamaterials. More importantly, the nonlinear medium

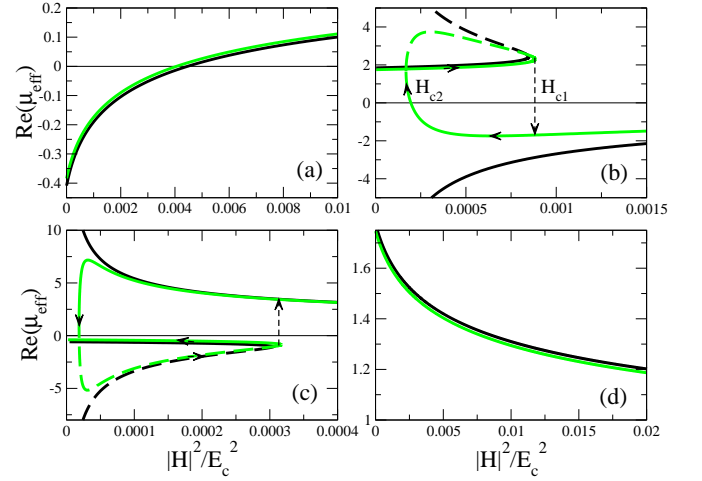


FIG. 1: Real part of the effective magnetic permeability vs. intensity of the magnetic field: (a)  $\Omega > 1$ ,  $\alpha = 1$ ; (b)  $\Omega < 1$ ,  $\alpha = 1$ , (c)  $\Omega > 1$ ,  $\alpha = -1$ ; and (d)  $\Omega < 1$ ,  $\alpha = -1$ . Black – the lossless case ( $\gamma = 0$ ), grey—the lossy case ( $\gamma = 0.05$ ). Dashed curves show unstable branches.

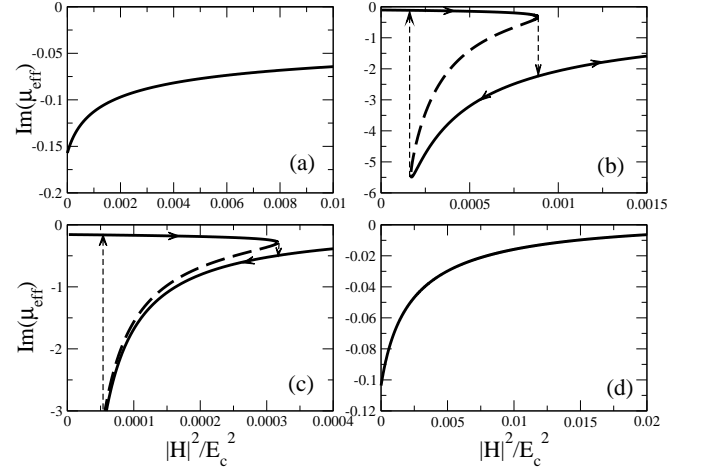


FIG. 2: Imaginary part of the effective magnetic permeability vs. intensity of the magnetic field for  $\gamma = 0.05$ : (a)  $\Omega > 1$ ,  $\alpha = 1$ ; (b)  $\Omega < 1$ ,  $\alpha = 1$ , (c)  $\Omega > 1$ ,  $\alpha = -1$ ; and (d)  $\Omega < 1$ ,  $\alpha = -1$ . Dashed curves show unstable branches.

can be created by inserting nonlinear elements into the slots of SRRs, allowing an easy tuning by an external field.

The critical fields for switching between LH and RH states, shown in the Figs. 1 can be reduced to a desirable value by choosing the frequency close to the resonant frequency of SRRs. Even for a relatively large difference between the SRR eigenfrequency and the external frequency, as we have in Fig. 1(b) where  $\Omega = 0.8$  (i.e.  $\omega = 0.8\omega_0$ ), the switching amplitude of the magnetic field is  $\sim 0.03E_c$ . The characteristic values of the focusing nonlinearity can be estimated for some materials such as n-InSb for which  $E_c = 200V/cm$  [13]. As a result, the strength of the critical magnetic field is found as  $H_{c1} \approx$

1.6A/m. Strong defocusing properties for microwave frequencies are found in  $\text{Ba}_x\text{Sr}_{1-x}\text{TiO}_3$  (see Ref. [14] and references therein). The critical nonlinear field of a thin film of this material is  $E_c = 4 \cdot 10^4 \text{V/cm}$ , and the corresponding field of the transition from the LH to RH state [see Fig. 1 (c)] can be found as  $H_c \approx 55.4 \text{A/m}$ .

The possibility of strongly enhanced nonlinearities in left-handed metamaterials revealed here may lead to an essential revision of the concepts based on the linear theory, since the electromagnetic waves propagating in such materials always have a finite amplitude. At the same time, the engineering of nonlinear composite materials will open a number of their novel applications such as frequency multipliers, beam spatial spectrum transformers, switches, limiters, etc.

### III. FDTD SIMULATIONS OF NONLINEAR METAMATERIAL

To study the electromagnetic wave scattering from the nonlinear metamaterial discussed above, we perform FDTD simulations of the plane wave interaction with the slab of LHM of finite size. We use the Maxwell's equations in the form

$$\begin{aligned} \text{rot} \vec{E} &= -\frac{1}{c} \frac{\partial \vec{B}}{\partial t}, \\ \text{rot} \vec{B} &= \frac{1}{c} \frac{\partial \vec{E}}{\partial t} + \frac{4\pi}{c} \langle \vec{j} \rangle + 4\pi \text{rot} \vec{M}, \end{aligned} \quad (2)$$

where  $\langle \vec{j} \rangle$  is the current density averaged over the period of the unit cell,  $\vec{M}$  is the magnetization of the metamaterial. The constitutive relations can be written in the form [15]

$$\begin{aligned} \sigma L_w S \frac{d \langle \vec{j} \rangle}{dt} + \langle \vec{j} \rangle &= \frac{\sigma S}{d_{\text{cell}}^2} \vec{E}, \\ \vec{M} &= \frac{n_m}{2c} \pi a^2 I_R \frac{\vec{B}}{|\vec{B}|}, \end{aligned} \quad (3)$$

where  $L_w$  is the inductance of the wire per unit length,  $\sigma$  is the conductivity of metal in the composite,  $S$  is the effective cross-section of a wire,  $S \approx \pi r_w^2$ , for  $\delta > r_w$ , and  $S \approx \pi \delta (2r - \delta)$ , for  $\delta < r_w$ , where  $\delta = c/\sqrt{2\pi\sigma\omega}$  is the skin-layer thickness,  $I_R$  is the current in SRR,  $n_m$  is concentration of SRRs. Current in SRRs is governed by the equation

$$L \frac{dI_R}{dt} = -\frac{\pi a^2}{c} \frac{dH'}{dt} - U - RI_R, \quad (4)$$

where  $L$  is inductance of the SRR,  $R$  is resistance of the SRR wire,  $U$  is the voltage on the SRR slit, and  $H'$  is the acting (microscopic) magnetic field, which differs from the average (macroscopic) magnetic field. Voltage

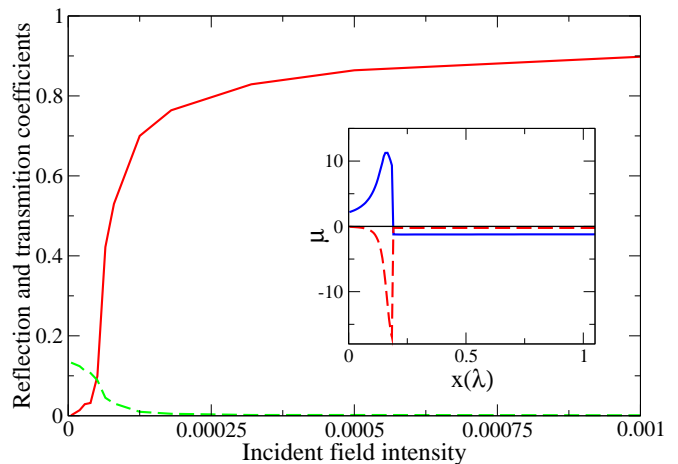


FIG. 3: Solid – reflection, dashed – transmission through the slab of metamaterial *vs* intensity of the incident field in a stationary regime. Inset shows real (solid) and imaginary parts of the magnetic permeability inside the slab of metamaterial. Defocussing nonlinearity,  $\alpha = -1$ .

on the slit of SRR  $U$  is coupled to the current  $I$  through the equation

$$C(U) \frac{dU}{dt} = I_R, \quad (5)$$

with

$$C(U) = \pi r^2 \epsilon \left( 1 + \alpha |U|^2 / U_c^2 \right) / 4\pi d_g,$$

where  $\epsilon$  is the linear part of the permittivity of a dielectric infilling the SRR slit,  $U_c$  is the characteristic nonlinear voltage, and  $\alpha = \pm 1$  corresponds to the focusing and defocusing nonlinearity.

The microscopic magnetic field  $H'$  can be expressed in terms of  $\vec{M}$  and  $\vec{B}$  using the Lorenz-Lorentz relation [16]:

$$H' = \vec{B} - \frac{8\pi}{3} \vec{M}. \quad (6)$$

As a result, Eqs.(2-6) form a closed system of equations and it can be solved numerically using FDTD method. Note, that substituting harmonic fields in this system of equations, one can find expression for the magnetic permeability (1).

To study the temporal dynamics of the wave scattering on the nonlinear metamaterial we consider 1D problem, which describes interaction of the plane wave incident at normal angle from air on a slab of metamaterial of finite thickness. We consider two types of nonlinear effects: (i) nonlinear darkening, when initially transparent left-handed material becomes opaque, and (ii) nonlinear induced transparency, when the opaque metamaterial becomes left-handed transparent. The first case corresponds to the dependence of the effective magnetic permeability on the external field shown in Figs. 1(a, c), when initially negative magnetic permeability (we consider  $\epsilon$  negative in all frequency range under study),

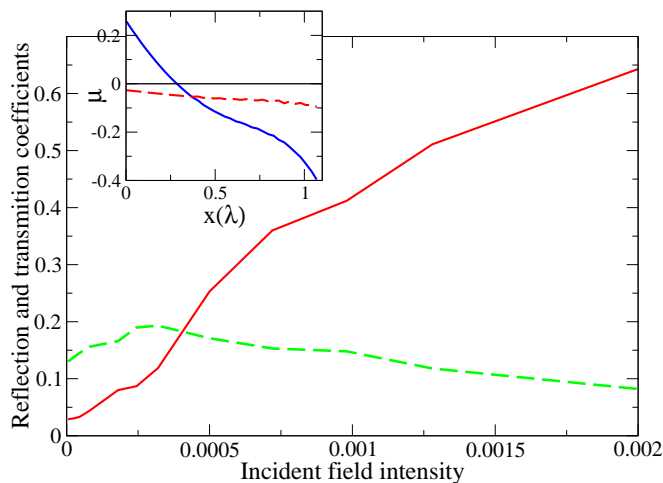


FIG. 4: Solid – reflection, dashed – transmission through the slab of metamaterial *vs* intensity of the incident field in a stationary regime. Inset shows real (solid) and imaginary parts of the magnetic permeability inside the slab of metamaterial. Focussing nonlinearity,  $\alpha = 1$ .

becomes positive with increase of the intensity of the magnetic field. The second case corresponds to the dependence of the magnetic permeability on external field shown in Figs. 1(b).

In all simulations we use linearly increasing amplitude of the incident field within first fifty periods of wave, and constant afterwards. The slab thickness equals to  $1.3\lambda_0$  where  $\lambda_0$  is a free-space wavelength. We have taken the material parameters so that the metamaterial is left-handed in linear regime in the frequency range from  $f_1 = 5.787$  GHz to  $f_2 = 6.05$  GHz.

Our simulations have shown that for the incident wave with the frequency  $f_0 = 5.9$  GHz (i.e. inside the left-handed transmission band), independently of the sign of the nonlinearity, electromagnetic field reaches the steady state. The *stationary* reflection and transmission coefficients as a function of the incident field amplitude are shown in Figs. 3,4 for defocussing and focussing nonlinear properties of the dielectric infilling SRR slits. We note, that in linear regime, parameters of the metamaterial on the frequency  $f_0$  are  $\epsilon = -1.33 - 0.01i$  and  $\mu = -1.27 - 0.3i$ , providing excellent impedance matching with surrounding air. It results in vanishing reflection coefficient for small incident field intensities (see Figs. 3,4).

Structure of the reflection and transmission coefficients is qualitatively different for various types of infilling nonlinear dielectric. For defocussing nonlinearity the reflection coefficient is switching from low to high level, when the incident field becomes larger than some threshold value (see Fig. 3). Such transition can be explained in terms of hysteresis behavior of the magnetic permeability shown in Fig. 1(c). When the field amplitude in metamaterial becomes higher than the critical amplitude (shown by the dashed arrow in Fig. 1(c)), magnetic permeability

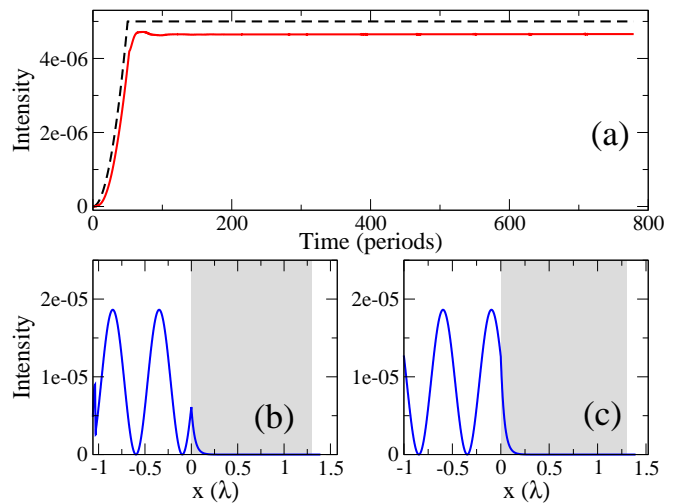


FIG. 5: (a) Solid – reflected, dashed – incident wave intensity *vs* time for small incident field amplitude (linear regime). (b),(c) magnetic and electric fields distribution at the end of simulation time, the region of metamaterial is shaded.

becomes positive, and the metamaterial becomes opaque. Our FDTD simulations show that for overcritical amplitudes of the incident field, the opaque region of positive magnetic permeability appears inside the slab (see inset in Fig. 3). We note that the magnetic permeability experiences abrupt change on the boundary between transparent and opaque regions. The dependencies shown in Fig. 3 were obtained, when the incident field increased from zero to the steady state value, as discussed above. However, taking different temporal behavior of the incident wave, e.g. increasing it above the threshold value and then decreasing it to the steady state, one can get different values of the stationary reflection and transmission coefficients, and different distributions of the magnetic permeability inside the slab of LHM. Such properties of the nonlinear metamaterial slab are consistent with multi-valued dependence of the magnetic permeability on the amplitude of the magnetic field.

In the case of focussing nonlinearity (see Fig. 4), we have a smooth dependence of the reflection and transmission coefficients on the amplitude of the incident field. Such behavior results, firstly, from the gradual detuning from the impedance matching condition, and, for higher powers, from the appearance of the opaque layer (see inset in Fig. 4) with positive magnetic permeability. Magnetic permeability in this case is a continuous function of the coordinate inside the slab.

Now we consider the case, when initially opaque metamaterial becomes transparent with increase of the amplitude of the incident field. We take the frequency of the incident field to be  $f_0 = 5.67$  GHz, so that in linear regime magnetic permeability is positive, and the metamaterial is opaque. In the case of  $\alpha = 1$ , or self-focussing properties on dielectric it is possible to switch to the regime with negative magnetic permeability (see Fig.1(b)) and make

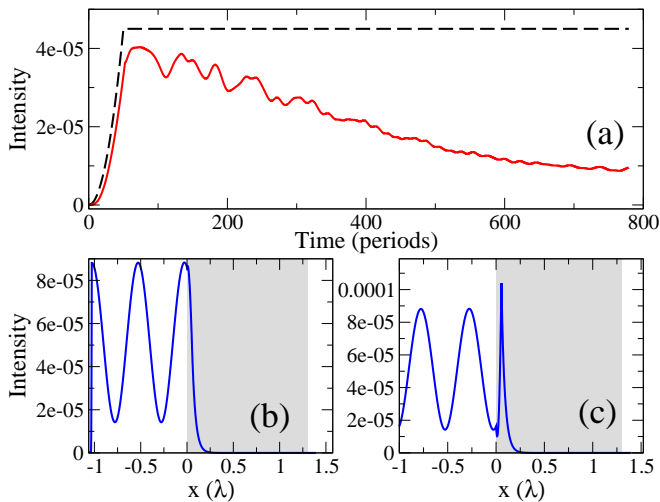


FIG. 6: (a) Solid – reflected, dashed – incident wave intensity *vs* time for overcritical incident wave amplitude. (b),(c) magnetic and electric fields distribution at the end of simulation time, the region of metamaterial is shaded.

the material left-handed transparent. Moreover, one can expect the possibility of formation of localized states inside the composite, the effect which was previously discussed for the interaction of the intense electromagnetic waves with overdense plasma [17]. Figure 5(a) shows dependence of the incident and reflected wave intensities as a function of time for small input intensities, which corresponds to the linear regime. The reflection reaches the steady state after approximately 100 periods. Electric and magnetic field profiles at the end of simulations are shown in Fig. 5(b,c).

In a weakly overcritical regime (see Fig. 6), the intensity of the reflected beam decreasing while approaching to the steady state. In this case we note the formation of the localized state in the vicinity of the metamaterial edge, (as can be seen more distinctly on Fig. 6(c)), which provides additional absorption of the electromagnetic energy, thus decreasing the reflection coefficient.

In the strongly overcritical regime (see Fig. 7), we observe dynamical self-modulation of reflected electromagnetic wave, which results from periodic formation of the self-localized states inside the metamaterial. Such localized states resemble temporal solitons, which transfer the energy away from the interface. Fig. 7(c) shows two localized states inside the metamaterial. These localized states appear on the jumps of the magnetic permeability, and, as a result, we observe the change of the sign of the derivative of electric field at the maximum of the soliton intensity, and creation of the transparent regions of the metamaterial. Compared to all previous cases, field structure did not reach steady state for high enough intensities of the incident field.

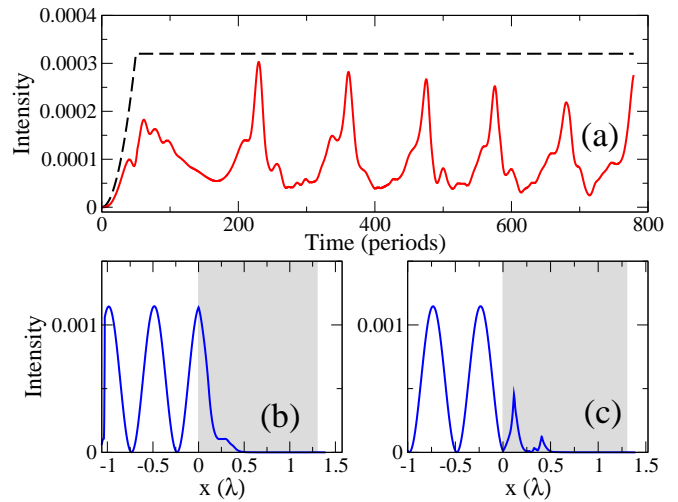


FIG. 7: (a) Solid – reflected, dashed – incident wave intensity *vs* time for strongly overcritical incident wave amplitude. (b),(c) magnetic and electric fields distribution at the end of simulation time, the region of metamaterial is shaded.

#### IV. ELECTROMAGNETIC SPATIAL SOLITONS

Nonlinear left-handed composite media can support self-trapped electromagnetic waves in the form of *spatial solitons*. Such solitons possess interesting properties because they exist in materials with a hysteresis-type (multi-stable) nonlinear magnetic response. Below, we describe novel and unique types of single- and multi-hump (symmetric, antisymmetric, or even asymmetric) backward-wave spatial electromagnetic solitons existing due to the effective domains of nonlinear magnetic permeability.

Spatially localized TM-polarized waves that are described by one component of the magnetic field and two components of the electric field. Monochromatic stationary waves with the magnetic field component  $H = H_y$  propagating along the  $z$ -axis and homogeneous in the  $y$ -direction,  $[\sim \exp(i\omega t - ikz)]$ , are described by the dimensionless nonlinear Helmholtz equation

$$\frac{d^2 H}{dx^2} + [\epsilon\mu(|H|^2) - \gamma^2]H = 0, \quad (7)$$

where  $\gamma = kc/\omega$  is a wavenumber,  $x = x'\omega/c$  is the dimensionless coordinate, and  $x'$  is the dimensional coordinate. Different types of localized solutions of Eq. (7) can be analyzed on the phase plane  $(H, dH/dx)$  (see, e.g., Refs. [18]). First, we find the equilibrium points: the point  $(0, 0)$  existing for all parameters, and the point  $(0, H_1)$ , where  $H_1$  is found as a solution of the equation

$$X^2(H_1) = X_{\text{eq}}^2 = \Omega^2 \left\{ 1 + \frac{F\epsilon_{\text{eff}}}{(\gamma^2 - \epsilon_{\text{eff}})} \right\}. \quad (8)$$

Below the threshold, i.e. for  $\gamma < \gamma_{\text{tr}}$ , where  $\gamma_{\text{tr}}^2 = \epsilon[1 + F\Omega^2/(1 - \Omega^2)]$ , the only equilibrium state  $(0, 0)$

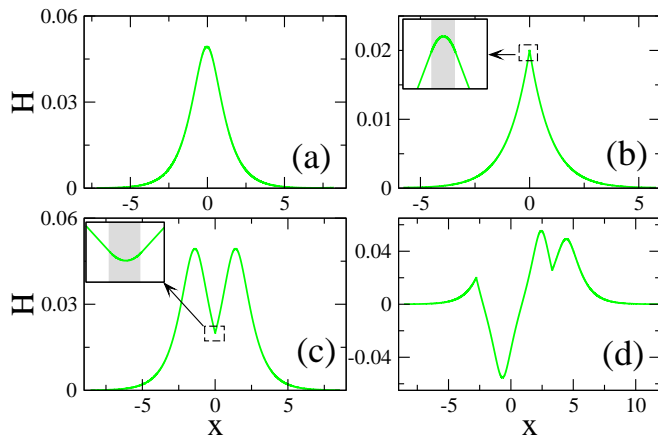


FIG. 8: Examples of different types of solitons: (a) fundamental soliton; (b,c) solitons with one domain of negative or positive magnetic permeability (shaded), respectively; (d) soliton with two different domains (shaded). Insets in (b,c) show the magnified regions of the steep change of the magnetic field.

is a saddle point and, therefore, no finite-amplitude or localized waves can exist. Above the threshold value, i.e. for  $\gamma > \gamma_{\text{tr}}$ , the phase plane has three equilibrium points, and a separatrix curve corresponds to a soliton solution.

In the vicinity of the equilibrium state  $(0, 0)$ , linear solutions of Eq. (7) describe either exponentially growing or exponentially decaying modes. The equilibrium state  $(0, H_1)$  describes a finite-amplitude wave mode of the transverse electromagnetic field. In the region of multi-stability, the type of the phase trajectories is defined by the corresponding branch of the multi-valued magnetic permeability. Correspondingly, different types of the spatial solitons appear when the phase trajectories correspond to the different branches of the nonlinear magnetic permeability.

The fundamental soliton is described by the separatrix trajectory on the plane  $(H, dH/dx)$  that starts at the point  $(0, 0)$ , goes around the center point  $(0, H_1)$ , and then returns back; the corresponding soliton profile is shown in Fig. 8(a). More complex solitons are formed when the magnetic permeability becomes multi-valued and is described by several branches. Then, soliton solutions are obtained by switching between the separatrix trajectories corresponding to different (upper and lower) branches of magnetic permeability. Continuity of the tangential components of the electric and magnetic fields at the boundaries of the domains with different values of magnetic permeability implies that both  $H$  and  $dH/dx$  should be continuous. As a result, the transitions between different phase trajectories should be continuous.

Figures 8(b,c) show several examples of the more complex solitons corresponding to a single jump to the lower branch of  $\mu(H)$  (dotted) and to the upper branch of  $\mu(H)$

(dashed), respectively. The insets show the magnified domains of a steep change of the magnetic field. Both the magnetic field and its derivative, proportional to the tangential component of the electric field, are continuous. The shaded areas show the effective domains where the value of magnetic permeability changes. Figure 8(d) shows an example of more complicated multi-hump soliton which includes two domains of the effective magnetic permeability, one described by the lower branch, and the other one – by the upper branch. In a similar way, we can find more complicated solitons with different number of domains of the effective magnetic permeability.

We note that some of the phase trajectories have discontinuity of the derivative at  $H = 0$  caused by infinite values of the magnetic permeability at the corresponding branch of  $\mu_{\text{eff}}(H)$ . Such a non-physical effect is an artifact of the lossless model of a left-handed nonlinear composite considered here for the analysis of the soliton solutions. In more realistic models that include losses, the region of multi-stability does not extend to the point  $H = 0$ , and in this limit the magnetic permeability remains a single-valued function of the magnetic field [8].

For such a multi-valued nonlinear magnetic response, the domains with different values of the magnetic permeability "excited" by the spatial soliton can be viewed as effective induced left-handed waveguides which make possible the existence of single- and multi-hump soliton structures. Due to the existence of such domains, the solitons can be not only symmetric, but also antisymmetric and even asymmetric. Formally, the size of an effective domain can be much smaller than the wavelength and, therefore, there exists an applicability limit for the obtained results to describe nonlinear waves in realistic composite structures.

When the infilling dielectric of the structure displays *self-focusing nonlinear response*, we have  $\Omega < 1$ , and in such system we can find *dark solitons*, i.e. localized dips on the finite-amplitude background wave [19]. Similar to bright solitons, there exist both fundamental dark solitons and dark solitons with domains of different values of magnetic permeability. For self-defocusing nonlinearity and  $\Omega < 1$ , magnetic permeability is a single-valued function, and such a nonlinear response can support dark solitons as well, whereas for self-focusing dielectric, we have  $\Omega > 1$  and no dark solitons can exist.

In conclusion, we have analyzed nonlinear response of left-handed metamaterials. For the harmonic fields we have calculated effective magnetic permeability and predicted hysteresis behavior of the magnetic permeability as a function of applied magnetic field. We have studied temporal dynamics of the wave reflection from the slab of nonlinear metamaterial using FDTD simulations. Finally, we predicted the existence of electromagnetic spatial solitons supported by the hysteresis-type nonlinear magnetic permeability.

- 
- [1] J.B. Pendry, A.J. Holden, W.J. Stewart, and I. Youngs, Phys. Rev. Lett. **76**, 4773 (1996).
- [2] J.B. Pendry, A.J. Holden, D.J. Robbins, W.J. Stewart, IEEE Trans. Microwave Theory Tech. **47**, 2075 (1999).
- [3] P. Markos and C.M. Soukoulis, Phys. Rev. E **65**, 036622(2002); Phys. Rev. B **65**, 033401 (2002).
- [4] D.R. Smith, W. Padilla, D.C. Vier, S.C. Nemat-Nasser, and S. Shultz, Phys. Rev. Lett. **84**, 4184 (2000).
- [5] M. Bayindir, K. Aydin, E. Ozbay, P. Markos, and C. M. Soukoulis, Appl. Phys. Lett. **81**, 120 (2002).
- [6] C.G. Parazzoli, R.B. Greigor, K. Li, B.E.C. Koltenbah, and M. Tanielian, Phys. Rev. Lett. **90**, 107401 (2003).
- [7] V. G. Veselago, Sov. Phys. Uspekhi **8**, 2854 (1967) [Sov. Phys. Usp. **10**, 509 (1968)].
- [8] A.A. Zharov, I.V. Shadrivov, and Yu.S. Kivshar, Phys. Rev. Lett. **91**, 037401 (2003).
- [9] M. Lapine, M. Gorkunov, and K.H. Ringhofer, Phys. Rev. E **67**, 065601 (2003).
- [10] C. Luo, S.G. Johnson, and J. D. Joannopoulos, Appl. Phys. Lett. **83**, 2352 (2002).
- [11] C. Luo, S.G. Johnson, J.D. Joannopoulos, J.B. Pendry, Phys. Rev. B **65**, 201104(R) (2002).
- [12] M. Gorkunov, M. Lapine, E. Shamonina, and K.H. Ringhofer, Eur. Phys. J. **B 28**, 263 (2002).
- [13] A. M. Belyantsev, V. A. Kozlov and V. I. Piskaryov, Infrared Physics **21**, 79 (1981).
- [14] H. Li, A. L. Roytburd, S. P. Alpay, T. D. Tran, L. Salamanca-Riba, and R. Ramesh”, Appl. Phys. Lett. **78**, 2354 (2001).
- [15] I.V. Shadrivov, N.A. Zharova, A.A. Zharov, and Yu.S. Kivshar, Phys. Rev. E, **4** (2004), in press.
- [16] M. Born and E. Wolf, *Principles of Optics: Electromagnetic Theory of Propagation, Interference and Diffraction of Light* (Cambridge University Press, UK, 2002).
- [17] K. Zauer, L. M. Gorbunov, Fizika Plazmy, **3**, 1302 (1977) (in Russian); A. A. Zharov, A. K. Kotov, Fizika Plazmy, **10**, 615 (1984) (in Russian); A. V. Kochetov, A. M. Feigin, Fizika Plazmy, **14**, 716 (1988) (in Russian).
- [18] V. B. Gil'denburg, A. V. Kochetov, A. G. Litvak, and A. M. Feigin, Sov. Phys. JETP **57**, 28 (1983) [Zh. Eksp. Teor. Fiz. **84**, 48 (1983)].
- [19] For a comprehensive overview of spatial solitons in nonlinear optics, see Yu.S. Kivshar and G.P. Agrawal, *Optical Solitons: From Fibers to Photonic Crystals* (Academic Press, San Diego, 2003), 560 pp.